ELSEVIER

Journal of Crystal Growth 232 (2001) 473–480

JOURNAL OF CRYSTAL GROWTH

www.elsevier.com/locate/jcrysgro

Influence of gravity on post-nucleation transport in liquid/liquid diffusion chamber of protein crystallization

H.-X. Cang, R.-C. Bi*

Institute of Biophysics, Chinese Academy of Sciences, Beijing 100101, People's Republic of China

Abstract

Based on a space experiment of lysozyme crystallization, a two-dimensional model was designed to study numerically the post-nucleation transport in the liquid/liquid diffusion crystallization of proteins. The initial concentration distributions for protein and salt were calculated with a purely diffusive process before nucleation. The results of simulation show that a noticeable depletion zone of protein also exists around a growing crystal in liquid/liquid diffusion chamber under $0g$ condition. The gravity-driven convection decreases the thickness of the depletion zone seriously. Furthermore, influenced by the solutal convection, the protein concentration and solution supersaturation at the crystal/solution interface are much higher in $1g$ case than in $0g$ case. In addition, in our case the computed gravity-driven convection had more complicated pattern and higher strength than those known for the batch and vapor diffusion crystallizations. Our simulation also shows that the uniformity of concentration and supersaturation distributions at the crystal/solution interface could be improved by the gravity-driven convection. The lower uniformity in $0g$ case is owing to the initial gradient distribution of protein concentration in liquid/liquid diffusion crystallization, but it could be improved by adjusting the initial conditions of protein crystallization. © 2001 Elsevier Science B.V. All rights reserved.

Keywords: A1. Biocrystallization; A1. Convection; A1. Computer simulation; A2. Microgravity conditions; B1. Biological macromolecules; B1. Lysozyme

1. Introduction

The environment of microgravity in space could improve the quality of protein crystals [1]. It is intuitively obvious that the elimination of the gravity-induced solutal convection and the sedimentation of crystals should be responsible for the quality improvement of the space-grown crystals. But it was not clear how the solutal convection influences the protein crystal growth [2]. To date, the accumulation of the space experiments and ground-based studies give us better understanding of the effects of gravity on protein crystal growth. The gravity-induced solutal convection influences the protein crystal growth mainly through modifying the bulk transport of solutes and the interface kinetics [3–7]. The convection promotes the transport of solutes and the impurities, and increases the solute supersaturation and the impurity concentration at the crystal/solution (C/S) interface, but decreases the thickness of the depletion zone. It is generally

*Corresponding author. Tel.: +86-10-6488-9866; fax: +86-10-6487-1293.

E-mail address: rcbi@iname.com (R.-C. Bi).

0022-0248/01/$ - see front matter © 2001 Elsevier Science B.V. All rights reserved.
PII: S0022-0248(01)01080-6

accepted that the quality improvement of the protein crystals grown in space benefits from the solute depletion zone around the growing crystals [8].

Considering the importance of the diffusive–convective transport for understanding the gravity effects on protein crystal growth, it is necessary to do more studies on them. The numerical simulation is a powerful method to do this work. Among the three most important methods of protein crystal growth, the vapor diffusion (VD) and batch crystallizations have been studied in detail by this kind of methods [3,4]. As for the liquid/liquid diffusion (L/LD), which is considered more promising for space protein crystallization, the published studies mainly concentrate on the pre-nucleation transport [9–11], but few on the post-nucleation transport. The knowledge provided by the studies is insufficient for clearly understanding our space experiment with the L/LD method [12]. The L/LD method is obviously different from the VD and batch methods. So, the numerical studies on L/LD were conducted in our laboratory. Our simulation on the pre-nucleation transport has shown that L/LD method has a potential advantage of self-regulation [11], which is not used determindely till now. Here the numerical study on the post-nucleation process is presented, which uses initial conditions derived from our simulation of pre-nucleation transport. It has been found that the diffusive–convective transport may be more complex compared to those in vapor diffusion and batch crystallization.

2. Methods

2.1. Physical model

A two-dimensional (2D) Cartesian model was considered in order to carry out the simulation with a microcomputer. It is definite that a three-dimensional (3D) model could give a more realistic scene of the transport. However, a reasonable 2D model should be able to give a good approximation, as shown by the numerical simulation of batch crystallization [4]. The geometry of the physical model is shown in Fig. 1, which is based on the setup of our space experiment. The crystallization system is lysozyme/sodium chloride, in 0.1 M acetate buffer, at pH 4.5. The constant solute diffusivities and no cross intercoupling between the diffusive solute fluxes are assumed. However, because of the appearance of crystals in the crystallization chamber in this period, some of the original assumptions in the pre-nucleation simulation are no longer valid, and a few new conditions should be proposed.

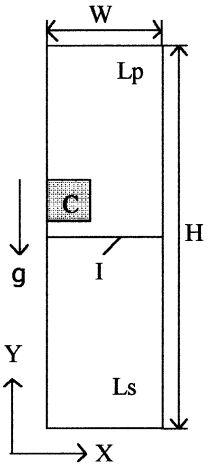

Fig. 1. Model of the liquid/liquid diffusion chamber, $H = 20$ mm and $W = 3$ mm. Symbols Lp, Ls, C, I and g represent protein solution, salt solution, crystal seed, original interface and gravity acceleration, respectively.

It is known that the crystals would emerge some time after the onset of the diffusion. At that time, the solute concentrations change continuously in the y-direction but are still uniform in the x-direction while the liquid/liquid interface has vanished. As protein crystals are very small and grow quite slow, the released crystallization enthalpy along with the nucleation and growth of the crystals could be ignored. Thus, the system is assumed isothermal (291 K) throughout the experiment.

Two problems concerning nucleation should be solved before the computation. One is the waiting time for nucleation. Our experiments showed that the microcrystals were observed about 10 h after the beginning of the experiment under the crystallization conditions used here. So a seed crystal was

put in the chamber 10 h after the activation of the experiment. Another is the location of the nucleus. It is known from the studies of the pre-nucleation process that there is a region with the maximum supersaturation in the protein solution. This region should have the highest probability of nucleation, which has been confirmed by our results of gelled protein crystallization [12]. So, the seed crystal was put in the region with the highest time-averaged supersaturation. The seed crystal was put at the side wall of the chamber as the nucleation often occurs at the container wall. This assumption could make the simulation more realistic and simpler by avoiding the sedimentation of the crystal during the crystal growth.

In our computation, the dimension of the seed crystal was taken as 0.6×0.6 mm. The seed crystal covers the area enclosed by lines $x = 0$, 0.6 mm and $y = 11.4$, 12 mm.

Here, one might argue that the Rayleigh–Bénard convection may occur before the nucleation. If that is true, then our following treatments would be inapplicable. Under the experimental conditions used in our case, the Rayleigh–Bénard convection would not occur, because as estimated, the density of the protein solution in the upper part is lighter than the density of the precipitant solution in the lower part before the crystal seed is put on. Afterwards, though the density of the upper solution would eventually exceed the density of the lower solution at some time, another necessary condition for the occurrence of the Rayleigh–Bénard convection, i.e. a static fluid, is no longer tenable as the growth of the crystal seed would generate the solutal convection.

2.2. Basic equations

To compute the diffusive–convective transport of the solutes in the post-nucleation process, two-dimensional equations are needed. With the Boussinesq approximation for fluid density, the basic equations are as follows:

$$\text{continuity equation:}\quad \frac{\partial u}{\partial x}+\frac{\partial v}{\partial y}=0, \tag{1}$$

momentum equation:

$$x\text{-direction:}\quad \frac{\partial u}{\partial t}+\frac{\partial (uu)}{\partial x}+\frac{\partial (uv)}{\partial y} = -\frac{1}{\rho_0}\frac{\partial p}{\partial x}+v\left(\frac{\partial^2 u}{\partial x^2}+\frac{\partial^2 u}{\partial y^2}\right), \tag{2}$$

$$y\text{-direction:}\quad \frac{\partial u}{\partial t}+\frac{\partial (uv)}{\partial x}+\frac{\partial (vv)}{\partial y} = -\frac{1}{\rho_0}\frac{\partial p}{\partial y}+v\left(\frac{\partial^2 v}{\partial x^2}+\frac{\partial^2 v}{\partial y^2}\right)-\frac{\rho}{\rho_0}\boldsymbol{g}, \tag{3}$$

$$\text{diffusion equation:}\quad \frac{\partial C_i}{\partial t}+\frac{\partial (uC_i)}{\partial x}+\frac{\partial (vC_i)}{\partial y} = D_i\left(\frac{\partial^2 C_i}{\partial x^2}+\frac{\partial^2 C_i}{\partial y^2}\right), \tag{4}$$

where u and v are the solutal convection velocity in the x- and y-direction, respectively; C_i and D_i, the concentration and diffusion coefficient of the solute, $i = \mathrm{p}$ for protein and $i = \mathrm{s}$ for salt; v, the kinematic viscosity; ρ_0 and ρ, the average and local solution densities, respectively; $\boldsymbol{g}$, the gravitational acceleration.

For two kinds of solutes, such as protein and salt here, the item ρ/ρ_0 in Eq. (3) should be

$$\rho/\rho_0 = 1+\beta_{\mathrm{p}}(C_{\mathrm{p}}-C_{\mathrm{p}}^0)+\beta_{\mathrm{s}}(C_{\mathrm{s}}-C_{\mathrm{s}}^0) \tag{5}$$

in which β_{p}, β_{s} are the coefficients of solutal expansion.

Eqs. (1)–(4) should be solved simultaneously. The method of stream-function/vorticity was used to compute their solutions. Stream-function ϕ and vorticity ω are generally defined by

$$u = \partial\phi/\partial y, \tag{6}$$

$$v = -\partial\phi/\partial x, \tag{7}$$

$$\omega = \partial v/\partial x - \partial u/\partial y, \tag{8}$$

Substituting Eqs. (6) and (7) into Eq. (8), one obtains

$$\partial^2\phi/\partial x^2 + \partial^2\phi/\partial y^2 = -\omega. \tag{9}$$

Using Eqs. (6)–(9), Eqs. (1)–(3) could be reduced to

$$\frac{\partial\omega}{\partial t}+\frac{\partial(u\omega)}{\partial x}+\frac{\partial(v\omega)}{\partial y} = v\left(\frac{\partial^2\omega}{\partial x^2}+\frac{\partial^2\omega}{\partial y^2}\right)-\sum_i \beta_i\frac{\partial C_i}{\partial x}\boldsymbol{g}. \quad (10)$$

2.2.1. Boundary conditions

There are no liquid slip and solute permeability at the chamber wall, which are expressed in equations:

$$x=(0,\ \mathrm{W}):\ \ \partial\phi/\partial x=\partial\phi/\partial y=0,$$

$$y=(0,\ L):\ \ \partial\phi/\partial y=\partial\phi/\partial x=0, \quad (11)$$

$$x=(0,\ \mathrm{W}):\ \ \partial C_i/\partial x=0,$$

$$y=(0,\ \mathrm{L}):\ \ \partial C_i/\partial y=0. \quad (12)$$

The stationary crystal/solution (C/S) interface was assumed [4]. Further experiments [13,14] showed that the relation between crystal growth velocity V_c and interfacial supersaturation σ is nonlinear. For simplicity, Pusey's result [15] was used here, which is

$$V_c=A(\sigma-1)^B, \quad (13)$$

$$\sigma=(C_p-C_p^S)/C_p^S \quad (13a)$$

in which A and B are dynamic coefficients; C_p^S is the protein solubility. Taking the average solution density as $1\,g/cm^3$, the boundary condition at the interface could be written as

$$(C_c-\rho_c C_p^I)V_c=-D_p\nabla C_p\cdot\mathbf{n}. \quad (14)$$

Here C_c is the protein concentration in the protein crystal; C_P^I is the protein concentration at the C/S interface.

2.2.2. Initial condition

As the crystals emerge about 10 h after the onset of the experiment, the initial conditions for the simulation of the post-nucleation period are not the initial conditions of the experiment. The initial concentrations of the solutes for the simulation were shown in Fig. 2, which were calculated with a pure diffusion process of pre-nucleation, with $C_p^0=25\,mg/ml$, $C_{ps}=3.75\%$, $C_S^0=15\%$ and the same volumes of protein and salt solutions. Here, C_p^0, C_S^0 and C_{ps} represent the initial protein concentration, salt concentration and salt concentration in the protein solution of the experiment, respectively. The physical parameters used in the computation were listed in Table 1. The data on lysozyme solubility were obtained from Ref. [17].

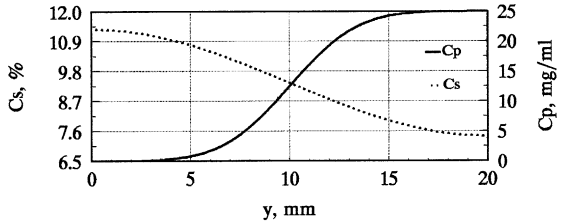

Fig. 2. Profiles of the initial concentrations of the solutes for the post-nucleation computation.

Table 1
The physical parameters used in computation

Parameter	Value	Reference
D_S	$1.47\times10^{-5}\,cm^2/s$	[4]
D_p	$1.00\times10^{-6}\,cm^2/s$	[4]
v	$0.012\,cm^2/s$	[16]
β_c	$2.94\times10^{-4}\,ml/mg$	[4]
β_S	5.96×10^{-3}	
C_c	820.0 mg/ml	[4]
A	$1.11\times10^{-9}\,cm/s$	[15]
B	2.08	[15]

2.3. Numerical scheme

To obtain the information on the fields of fluid flow, solute concentration and supersaturation, Eqs. (4), (6), (7), (9) and (10) should be solved iteratively, together with the boundary and initial conditions. An explicit finite-difference scheme was used to discretize the equations, in which the vorticity and diffusion items were discretized with central differencing scheme.

Considering the precision of the computation and the computing time, the mesh is non-uniform. The spatial step was 0.1 mm in the x-direction. In the y-direction, it changed from 0.1 mm in the vicinity of the seed crystal to 0.4 mm at the regions

near the top and bottom of the crystallization chamber. The temporal step was 0.001 s.

3. Results and discussion

With a computing program written in FORTRAN language, the solution flow, the concentration field and the supersaturation field were obtained for $1g$ and $0g$ cases. These results are presented below. The similarities and differences among the simulation results of L/LD, VD and batch crystallizations were also discussed.

3.1. Characteristics of solutal convection

Along with the growth of the seed crystal, the solutal convection emerged in the L/LD chamber under $1g$ condition. Fig. 3 shows the computed convection pattern and its evolution. It was found that the convection swirls arranged lengthways in the chamber. The swirl number increased with time elapsing. The convection strength also changed with time. In our computation, the maximum convection strength was 21.1 μm/s, located in the solution near the upright corner of the crystal. It decreased to about 16.4 μm/s 1 h later. The convection had more complicated pattern and a little higher strength than those known for the VD and batch crystallizations [3,4].

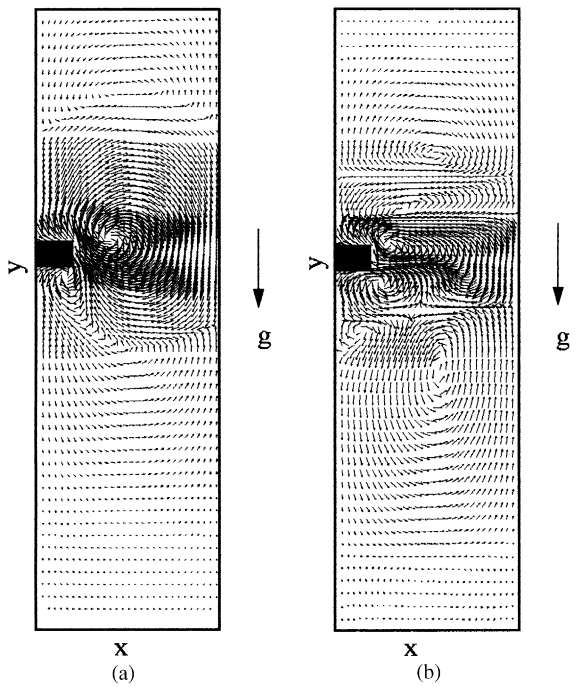

Fig. 3. Velocity vector fields of the solutal convection in $1g$ case after (a) 1 s and (b) 1 h of crystal growth.

Two factors might have big influence on the convection pattern and strength. One is the chamber geometry. The dimension of the L/LD chamber in our computation is 3×20 mm in width × height, which is different from those of the crystallization chambers used in the simulations of batch and VD crystallization. The larger size is favorable for the momentum transport of the fluid. The thin and high geometry of the L/LD chamber may make the swirls arranged lengthways. Another important factor is the initial distribution of the solutes. In our case the solutes have gradient distributions, and such non-uniform distributions also change with time. Although the evolution of the solute distributions would not result in the Rayleigh–Bénard convection, it might affect the convection pattern and strength. In addition, the protein crystal would prevent the protein diffusing downwards and the precipitant upwards, which would also influence the strength and pattern of the solutal convection.

3.2. Influence of convection on the field of protein concentration

The distributions of the protein concentration around the crystal in $1g$ and $0g$ cases are given in Fig. 4. It shows that the protein concentration has a sharp decrease in a narrow solution layer around the crystal under $1g$ condition, but it decreased gradually in a quite wide region under $0g$ condition. Such concentration boundary layer is the so-called depletion zone. To show the depletion zones more clearly, some profiles of protein concentration at the half height of the crystal after 1 min and 1 h of crystal growth are given in Fig. 5. The curves show that the thickness of the depletion zone is about a constant of 0.1 mm in $1g$ case. However, it increased to 1.5 mm within 1 h in $0g$ case. So, in L/LD case, the computed thickness of the depletion zones in $1g$ and $0g$ cases have the

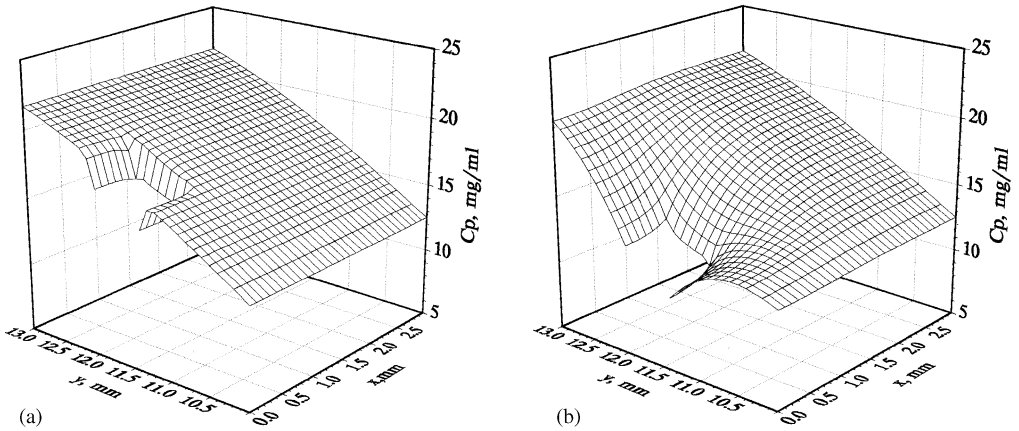

Fig. 4. Fields of protein concentration in the vicinity of the growing crystal in (a) 1g case and (b) 0g case after 1 h of crystal growth.

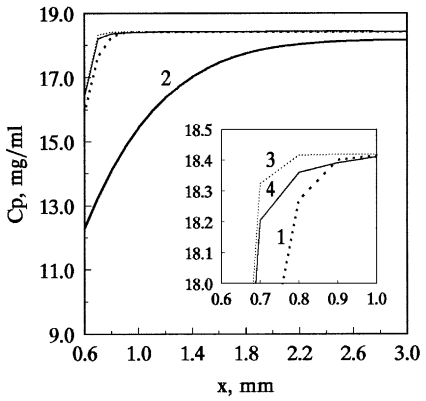

Fig. 5. Profiles of protein concentration in the solution at the half height of the crystal. The conditions corresponding to the curves are: curve 1—0g and 1 min; curve 2—0g and 1 h; curve 3—1g and 1 min; curve 4—1g and 1 h.

same orders of magnitude as that in batch crystallization [4], respectively.

Another point shown by Fig. 5 is that the protein concentration at the C/S interface in 1g case is higher than in 0g case. At the middle of right C/S interface, C_p^I kept about 16.5 mg/ml in 1g case, but it decreased to 12.3 mg/ml within 1 h in 0g case (Fig. 5).

It could also be seen from Fig. 5 that the curves are slightly different from those in batch crystallization at the same time: they intersect each other in the batch crystallization [4]; but do not for L/LD crystallization. In addition, the distribution of protein concentration at the C/S interface is more uniform in 1g case than in 0g case, i.e. the solutal convection could improve the distribution of the protein concentration at the C/S interface. This is also different from the situation of batch crystallization. These differences may be caused by the different initial distributions of protein concentration. In L/LD case, the pre-nucleation distribution of protein concentration is non-uniform, and there is a gradient distribution before nucleation.

3.3. Influence of convection on crystal growth

To investigate the influence of convection on protein crystal growth, the supersaturation was calculated from the solute concentrations. The distributions of supersaturation in 1g and 0g cases are similar to those of protein concentration under the same conditions, respectively. However, supersaturation is determined not only by protein concentration, but also by precipitant concentration. Examining the distribution of the precipitant concentration in the L/LD chamber, it was found that since the seed crystal was put in, the lowest precipitant concentration exceeds 7% located at the top of the solution. From the solubility curves of lysozyme, it is known that the solubility is low when the precipitant concentration exceeds 5%, and it decreases very slowly along with the increase

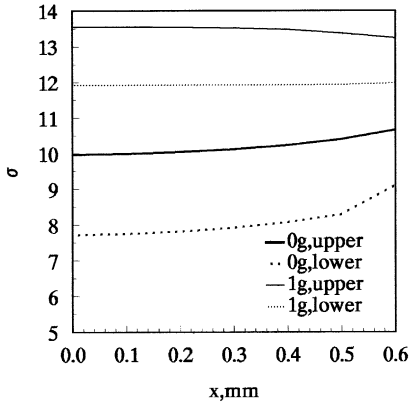

Fig. 6. Profiles of supersaturation at the upper and lower C/S interfaces in $1g$ and $0g$ cases after 1 h of crystal growth.

of precipitant concentration. As a result, the influence of the distribution of precipitant concentration on solution supersaturation is smaller, and the solution supersaturation relies mainly on protein concentration.

The supersaturation distributions at the C/S interface given in Fig. 6 show the non-uniformity of the supersaturation distributions in the case of given crystallization conditions. Influenced by the solutal convection, the supersaturation at the C/S interface is clearly higher in $1g$ case than in $0g$ case. Furthermore, the uniformity of the supersaturation distribution at the C/S interface is little improved by convection.

It is generally considered that the L/LD crystallization is more promising than other methods for protein crystallization in space. Nevertheless, as shown in our computation, the non-uniformity of supersaturation distribution might be present in $0g$ case. It is not likely to be improved even after a long time, such as 100 h or more, as the protein molecules diffuse very slowly.

Along with the accumulation of the space experiments and ground-based studies, it is known that the influencing mechanism of the gravity on protein crystal growth is quite complicated. According to the uniformity of the supersaturation distribution, the L/LD crystallization seems more applicable for the ground experiments. However, the higher interface supersaturation in the ground experiments corresponds to a larger growth rate and could produce worse crystal quality. There are also evidences showing that the enhanced convective supply of impurities to the C/S interface could cause the crystal defects [6]. As experiments revealed, the crystals grown in terrestrial condition incorporated higher amount of impurities than those grown in space [7]. On the contrary, the solutions would remain static in $0g$ case, and the depletion zone would be much thicker than in $1g$ case. The static diffusion field and the thicker depletion zone have a purifying effect by decreasing the opportunity of impurities to access the protein crystal [7,8]. Meanwhile, the thicker depletion zone in $0g$ case may eliminate the occurrence of new nucleus near the growing crystals. All of these aspects show that the protein crystallization in space should have more advantages than on the ground.

Furthemore, even the non-uniformity of the supersaturation distribution could be improved through adjusting the initial conditions of protein crystallization according to our results of numerical simulation on the pre-nucleation transport [11]. Our previous simulation has shown that there would be a supersaturation peak with the highest probability of nucleation when the initial conditions are adequate, e.g. there is no precipitant in the protein solution and large volume ratio of protein solution to precipitant solution. If protein crystals lie in the middle of the region where the supersaturation peak locates, the non-uniformity of supersaturation distribution at the C/S interface would be much improved.

4. Summary

Using a model based on a real space experiment, a numerical study was carried out for the post-nucleation transport in the L/LD crystallization of proteins. The initial field of solute concentration employed the concentration distribution, which obtained from a numerical simulation of pure-diffusion controlled pre-nucleation transport in the crystallization chamber used here.

The results of simulation have shown that a thicker depletion zone also exists around a growing crystal under $0g$ condition. The gravity-driven convection could decrease the thickness of

the depletion zone remarkably, and increase seriously the solute concentration around a growing crystal.

Compared to other cases with different methods of protein crystallization, the computed solutal convection has more complicated pattern and higher strength. This difference was analyzed to be due to the special geometry of L/LD chamber and the evolution of the specific solute distribution for L/LD method. In addition, in the presence of gradient distribution of solutes, gravity may improve the non-uniform distribution of solute concentration around crystals to some extent. However, the non-uniformity of supersaturation distribution at the C/S interface in $0g$ case could be reduced through adjusting the initial crystallization conditions.

References

[1] W. Littke, C. John, Science 225 (1984) 203.
[2] L.J. DeLucas, F.L. Suddath, R. Synder, R. Naumann, et al., J. Crystal Growth 76 (1986) 681.
[3] R. Savino, R. Monti, J. Crystal Growth 165 (1996) 308.
[4] H. Lin, F. Rosenberger, J.I.D. Alexander, A. Nadarajah, J. Crystal Growth 151 (1995) 153.
[5] P.G. Vekilov, F. Rosenberger, J. Crystal Growth 186 (1998) 251.
[6] P.G. Vekilov, F. Rosenberger, H. Lin, B.R. Thomas, J. Crystal Growth 196 (1999) 261.
[7] B.R. Thomas, A.A. Chernov, P.G. Vekilov, D.C. Carter, J. Crystal Growth 211 (2000) 149.
[8] A. McPerson, A.J. Malkin, Y.G. Kuznetsov, S. Koszelak, et al., J. Crystal Growth 196 (1999) 572.
[9] G. Wagner, R. Linhardt, J. Crystal Growth 110 (1991) 114.
[10] F. Otalora, J.M. Garcia-Ruiz, J. Crystal Growth 169 (1996) 361.
[11] H.-X. Cang, R.-C. Bi, J. Crystal Growth 194 (1998) 133.
[12] J.-S. Pan, X.-T. Niu, L.-L. Gui, R.-C. Bi, et al., J. Crystal Growth 168 (1996) 227.
[13] Kazuo Kurihara, Satoru Miyashita, Gen Sazaki, et al., J. Crystal Growth 166 (1996) 904.
[14] Y.G. Kuznetsov, A.J. Malkin, A. Greenwood, A. McPherson, J. Crystal Growth 166 (1996) 913.
[15] M. Pusey, R. Naumann, J. Crystal Growth 76 (1986) 593.
[16] W.J. Fredericks, M.C. Hammonds, S.B. Howard, F. Rosenberger, J. Crystal Growth 141 (1994) 183.
[17] E. Cacioppo, M.L. Pusey, J. Crystal Growth 114 (1991) 286.